Original Article

MiRNA-146a in Mesenchymal Stem Cells Exosome Alleviates Histological Structure of Pulmonary Tissue Via IRAK1 / NF-κB Pathway in Experimentally Induced Bronchial Asthma

Eman M. Mohamed and Mai A. Samak

Department of Medical Histology and Cell Biology, Faculty of Medicine, Zagazig University, Egypt

ABSTRACT

Introduction: Bronchial asthma is a multifaceted respiratory disorder that represents a significant global public health concern, afflicting millions of individuals and resulting in considerable morbidity and mortality.

Aim of Work: To unravel the intricate ultra-structural and cyto-molecular potential impacts of exosomes released by mesenchymal stem cells (MSCs) as biocompatible nanocarriers of miR-146 on experimentally induced bronchial asthma.

Materials and Methods: Thirty-two male adult albino rats were splitted into three groups. Group I (control group), group II (experimentally induced asthma group): Every rat got 25 µg house dust mite (HDM) extract suspended in 35 µL of saline for five sequential days weekly for four weeks intranasally, and group III (exosome-treated groups): rats were administered HDM as group II, and after two weeks, they received 100 µg MSC-derived exosomes in 0.5 ml PBS intravenous through the tail vein, once/day for two weeks. Pulmonary tissue samples were examined for histopathological, ultrastructural, and NF-κB immune expression beside RT-PCR estimation of miR-146a, IRAK1, and NF-κB.

Results: Observable morphological and ultrastructural restoration of pulmonary tissue architecture in the MSCs exosomes-treated group compared to induced asthma group were recorded. Furthermore, the significant suppression of IRAK1 and NF-κB, along with the expantion of miR-146a and reduced immunohistochemical representation of NF-κB in the exosomes-treated group, indicated the potential molecular mechanisms for the observed histo-morphometric impacts.

Conclusion: Our study outlined the therapeutic implicit of miRNA-146 in mesenchymal stem cell exosomes via IRAK1/NF-κB pathway as a novel and effective approach for managing bronchial asthma and paving the way for further research.

Received: 16 September 2023, **Accepted:** 15 November 2023

Key Words: Bronchial asthma, exosomes, histology, MiRNA-146a, IRAK1 / NF-κB.

Corresponding Author: Eman M. Mohamed, PhD, Department of Medical Histology and Cell Biology, Faculty of Medicine, Zagazig University, Egypt, **Tel.**: +966535648629, +201093634726, **E-mail:** emanmosallam79@gmail.com

ISSN: 1110-0559, Vol. 47, No. 4

INTRODUCTION

Bronchial asthma is a multifaceted respiratory disorder that manifests itself in various phenotypes yet shares certain common features, including inflammation and reversible airway obstruction. It represents a significant worldwide health concern, afflicting millions of individuals and resulting in considerable complications[1]. The evolution of asthma is ascribed to the complex interplay of allergens and epigenetic modifications that engender respiratory symptoms like coughing, wheezing, chest tightness, and variable airflow limitation[2]. Depending on the inflammatory status and molecular mechanisms involved, asthma can be classified into different phenotypes and endotypes, which can help clinicians to better characterize and treat the disease[3,4].

The pathogenesis of asthma is initiated by various inflammatory pathways and the differentiation and proliferation of specific T cells, which promote the production of various chemotactic factors like interleukin 4, 5, 13, and 17, in addition to growth factors[5,6]. Consequently, they result in the recruitment of eosinophils and neutrophils to the lungs and the emergence of various disease-associated factors such as airway constriction, smooth muscle thickening, fibrosis, airway remodeling, and hyperresponsiveness[7]. Advanced drug delivery systems, such as nanotherapeutics, offer a hopeful approach for targeting senescence and inflammasomes in asthmatics, whether in pre-clinical animal models or clinical studies[8].

Currently, there have been remarkable advancements in mesenchymal stem cell (MSC) research. However, despite many significant strides, several challenges remain to be addressed to fully harness MSCs for medicinal purposes[9]. Such challenges pertain to the size of MSCs that may encounter difficulties in traversing through narrow capillaries or probable risk of pulmonary embolism. Hence, ensuring the effectiveness and safety of MSC-based therapies necessitates addressing this concern comprehensively[10].

Continued research and technological advancements in MSCs offer hope for unlocking their full therapeutic potential and to overcome these challenges. Doing so can pave the way for the safe and effective clinical applications

DOI: 10.21608/ejh.2023.235299.1947

of MSCs in regenerative medicine. Furthermore, MSCs release extracellular vesicles (EVs), which are small membrane-bound vesicles containing bioactive particles such as proteins, lipids, and nucleic acids[11].

EVs have achieved significant attention from researchers because of their possible medical use. Firstly, they are highly stable, making them suitable for storage and transportation. Secondly, they are at low risk of immune rejection, as they lack the same surface markers as MSCs, reducing the probability of triggering an immune response. This makes them potentially suitable for allogeneic therapies. Thirdly, EVs from MSCs have demonstrated the competency to traverse the blood-brain barrier, facilitating their practical use in therapeutic applications[12,13].

Consequently, many investigators have shifted their focus toward studying and utilizing EVs from MSCs for medicinal purposes. The unique properties of MSC-extracted EVs make them appealing for drug release, tissue repair, modulation of the immune system, and other possible medical uses. Ongoing research in this area aims to deepen the understanding of MSCs' mode of action and optimize the usage of MSC-extracted EVs for medicinal purposes[14].

EVs exist in various sizes and types, including apoptotic bodies, exosomes/microvesicles, and the smallest type called exosomes[15]. Exosomes carry proteins, lipids, RNA, and DNA from their parent cells and are released into extracellular spaces to guide the behavior of other cells through paracrine signaling[16]. MicroRNAs (miRNAs) are eye-cashing exosomal products that can modify the behavior of nearby cells by adjusting gene expression and differentiation. MiRNAs are non-coding RNAs that impact various cell biological functions, inflammatory and redox pathways switching[17].

During the last decade, miRNAs proved several diagnostic, prognostic, and therapeutic applications; unique miRNA profiles proved association with specific types and stages of malignancies. They are also linked to tumor growth, invasion, and metastasis. Specific miRNA expression patterns can predict developing cardiovascular disorders such as heart failure or hypertension and confirm promise as therapeutic agents[18]. Furthermore, Dysregulation of miRNAs has been concomitant with different neurological ailments, involving Alzheimer's disease[19], Parkinson's disease[20], multiple sclerosis[21], and epilepsy[22].

The IRAK1/NF-κB pathway acts a crucial task in the innate immune response, enabling the immune system to react to infection, tissue damage, and other inflammatory stimuli[23]. It is named after its key components, interleukin-1 receptor-associated kinase 1 (IRAK1) and nuclear factor kappa B (NF-κB), which orchestrate its activities. Imbalance of this pathway can contribute to chronic inflammation spurt of different ailments, involving autoimmune disorders and various malignancies[24]. The task of miRNA-146a in adjusting the IRAK1/NF-κB pathway has been imputed in inflammatory diseases with paucity of scientific focus on bronchial asthma. Thereafter, we aimed to unravel the ultrastructural and cyto-molecular potential impacts of exosomes extracted from MSCs as biocompatible nanocarriers of miR-146 on experimentally induced bronchial asthma.

MATERIALS AND METHODS

Study animals

Thirty-two male adult albino rats (12–14 weeks, weighing 180–200 g) were held in cages in the Animal holding of the Faculty of Medicine, Zagazig University, Egypt. Animals were retained in a controlled environment and had ad libitum get of diet and liquid. Rats were cared for in concert with Ethical Committee guidelines from Zagazig University that guide the Use and Care of Laboratory Animals. The Institutional Animal Care and Use Committee, Zagazig University, Egypt, accepted the study (Protocol approval number: ZU-IACUC/3/F/173/2023).

Experimental design

After one week in the new area, three groups of rats were determined.

Group I (control group, 16 rats): Group Ia (8 rats) had no intervention, and group Ib (8 rats) exposed to intranasal instillation of 35 µL saline (dropwise, alternating between nostrils) for five consecutive days weekly for four weeks. After another two weeks, rats were injected with 0.5 ml phosphate-buffered saline (exosome vehicle) through the tail vein once/day for two weeks.

Group II (experimentally induced asthma group, eight rats): Every rat received 25 µg house dust mite (HDM) (Cat# XPB82D3A2.5, 2.5 ml/vial, Greer Laboratories, Lenoir, NC, USA through Thermo Fisher Scientific, San Jose, CA, USA) suspended in 35 µL of saline. Rats were sensitized for five sequential days weekly for four weeks intranasally (dropwise, alternating between nostrils)[25]. After two weeks of induced asthma (rats were injected with 0.5 ml phosphate-buffered saline (PBS) (exosome vehicle) through the tail vein once/day for two weeks.

Group III (exosome-treated group, eight rats): rats were administered HDM as group II, and after two weeks, they received 100 µg MSC-derived exosomes in 0.5 ml PBS intravenous through the tail vein, once/day for two weeks[26].

Preparation of MSC-derived exosomes

Exosomes were separated from MSCs which were cultured in Dulbecco's Modified Eagle Medium (DMEM) and 10% exosome-depleted fetal bovine serum (Sigma-Aldrich, St. Louis, MO, USA) for 48 h. The medium was then centrifuged many times to remove cells, as illustrated by[27]. Finally, the collected exosomes were suspended in PBS.

Sampling

Rats were sacrificed by cervical dislocation after intraperitoneal injection of sodium thiopental (50 mg/kg)[28] at the end of the experiments. The lungs were excised and dissected. Specimens from the lower left lobes of the lungs from each animal underwent histopathological analysis, whereas the lower right lobes were frozen in liquid nitrogen for real-time quantitative polymerase chain reaction (qPCR).

Molecular analysis

Real-time Polymerase Chain Reaction (RT-PCR)

RT-PCR has tested the mRNA representation for miR-146a, IRAK1, and NF-κB.

RNA was transcribed to cDNA. It was exposed to denaturation, annealing, and extension. For miRNAs, U6 was managed as an internal control for normalization. For mRNA, data were normalized against GAPDH.

The primer sequences used

miR- 146a, Forward: GGAACGATACAGAGAAGATTAGC

Reverse: TGGAACGCTTCACGAATTTGCG

IRAK1, Forward: CCCAGTGCTGGGGTAAGC

Reverse: TGTTCGCTCTACTGCAGACT

NF-κB, forward: 5′-AGAGCTAATCCGCCAAGCAG-3′,

Reverse: 5′-GACCTGTACTTCCAGTGCCC-3'

Histopathology

Light microscopy

Hematoxylin and eosin (H&E) staining

Specimens were fixed in buffered formalin and handled to form 5-μm-thick slices[29].

Immune histochemical staining

Avidin biotin–peroxidase complex method (Code No. K3954, Dako, Denmark) was accomplished for localization of NF-κB in the lung tissue. Dewaxing, hydration, and microwave treatment of paraffin sections was achieved. Endogenous peroxidase was removed, and nonspecific binding was blocked by a normal mice serum. Sections were covered with anti-NF-κB (Cat. No. #RB-9034-R7; 1/100 dilution; Thermo Scientific, USA). Secondary antibodies and labeled horseradish peroxidase were added. Staining at the antigen site by DAB appears brown[30].

Electron microscopy examinations

Tissue pieces were fixed in glutaraldehyde and osmium tetroxide. The processes were dehydration, embedding, ultra-cutting, and then staining in lead citrate and uranyl acetate[31]. Sections were photographed by TEM (JEOL JEM 1010, JEOL Ltd.) at Tanta University Faculty of Medicine.

Morphometric studies

The total number of immune-positive cells for anti-NF-κB was calculated using A Leica QWin 500 image analyzer computer system (Leica Ltd., Cambridge, UK).

The magnifications of inspected slides were 400. Five non-overlying areas were randomly chosen from every animal in every group and Measured by a blinded inspector.

Statistical analysis

SPSS version 22 (IBM Corp., Armonk, NY, USA) was used for data testing. Tukey's post hoc tests followed ANOVA tests. Probability values (p) < 0.05 were significant and highly significant at < 0.001.

RESULTS

Real-time qPCR

The exosome-treated group showed significant rises in miR-146a, and significant drop in IRAK1 and NF-κB ($p < 0.001$) levels relative to the experimentally induced asthma group. In contrast, no significant alterations were obtained relative to control group ($p > 0.05$) (Table 1).

Histopathological results

Results of H&E stain. Histological sections of H&E slides of control group showed Normal lung construction with rounded alveoli and alveolar sacs aligned by pneumocytes type 1 and 2 and separated by delicate inter-alveolar septa (Figures 1 A,B).

Segments of the experimentally induced asthma group revealed collapsed alveoli with thickened inter-alveolar septa. Marked inflammatory cellular penetration, engorged, dilated blood vessels with thick muscle coat, and fatty cellular infiltration in lung tissue were well observed. Extravasated erythrocytes appeared in the septa and the lumina of the alveoli, forming lung hemorrhage. Exfoliated bronchial epithelium into the lumen was obvious (Figures 2 A-E).

Sections of the exosome-treated group showed almost normal construction of the alveoli and bronchiolar structure. However, some alveoli appeared collapsed between the normal alveoli (Figures 3 A,B).

Results of Immune Histochemistry

NF-κB-stained tissues of control group displayed brown reactions in cytosol of scanty cells. Numerous cells were noted in the experimentally induced asthma group. Few reactions were still existing in the exosome-treated group (Figures 4 A-C).

Results of Electron microscope examination

Micrographs of ultrastructure of control group,s lung sections showed the alveolar lining by type 1 pneumocytes separated by delicate interalveolar septa, and type 2 pneumocytes presented with regular nuclei and lamellar bodies in their cytosol. (Figures 5 A,B). Pneumocytes

type 2 had regular nuclei with peripheral chromatin and nucleoli, lamellar bodies, and mitochondria (Figure 5C). Blood air barriers were made up of endothelial cells and thin type 1 pneumocyte cytoplasm with their adherent basal laminae (Figures 5 D,E).

Ultrastructure of sections from the experimentally induced asthma group unraveled thick inter-alveolar septa containing many connective tissue cells. Some cells appeared with pyknotic degenerated nuclei. Macrophages with pseudopodia and lysosomes were present in the septa (Figure 6A). Type 2 Pneumocytes were noted with irregular nuclei and empty lamellar bodies. An abundant amount of collagen fibers was also noticed (Figure 6B). Many cells appeared with rarified cytoplasm, vacuolations, and lysosomes (Figure 6C). the alveolar lumina housed exfoliated cells (Figure 6D). Some cells appear with dilated RER (Figure 6E). Eosinophils having dense granules were obvious in the interstitium which appeared with many collagen fibers (Figure 6F). Distorted blood air barriers, detached two basal lamina, many collagen fibers and wide cytosol of capillary endothelium were noticed (Figure 6G). Type I pneumocyte has a swollen cytoplasm and engorged blood capillary were observed in (Figure 6H).

Ultrastructure of sections from the exosome-treated group showed seemingly normal alveoli with delicate inter-alveolar septa. However, some cells appeared in the lumina (Figure 7A). Some cells of pneumocyte type 2 appeared with atypical indented nuclei. Some lamellar bodies also appeared vacuolated (Figure 7B). Nearly normal blood-air barriers were observed. They were made up of thin cytosols of endothelial cells and type I pneumocyte with their basal laminae were fused (Figure 7C).

Morphometric results

The calculated number of NF-κB immune representations got a big significant rise in the experimentally induced asthma group relative to control and exosome-treated groups. A significant rise in the exosome-treated group versus the control group was reached (p>0.05) (Table 2).

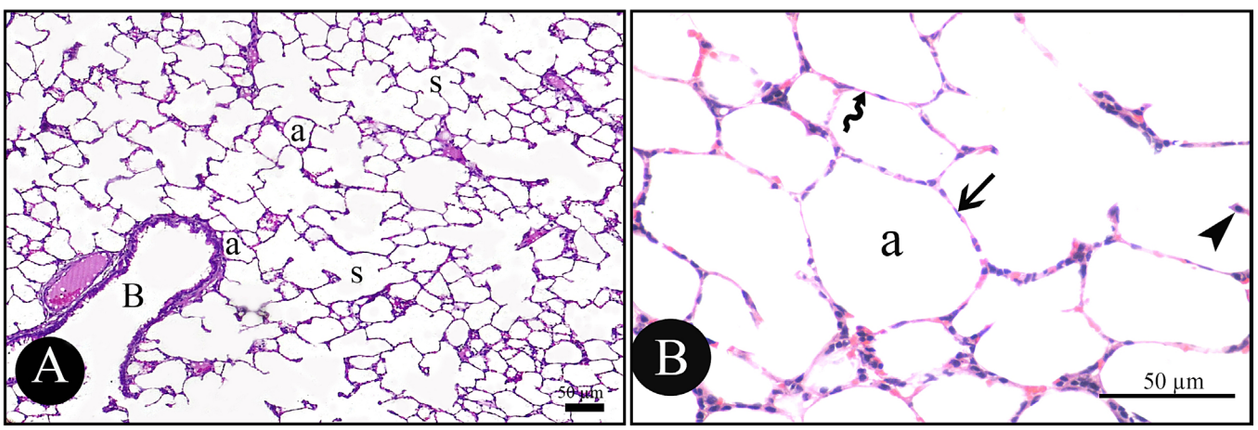

Fig. 1: Photomicrograph of histological sections of H&E slides of control group showing: (A): lung architecture with rounded alveoli (a), alveolar sacs (s) and a bronchiole (B) are observed. (B) The alveoli (a) are aligned by pneumocytes type 1 (arrows) and type 2 (arrow heads). The delicate interalveolar septa (zigzag arrows) separate the alveoli.

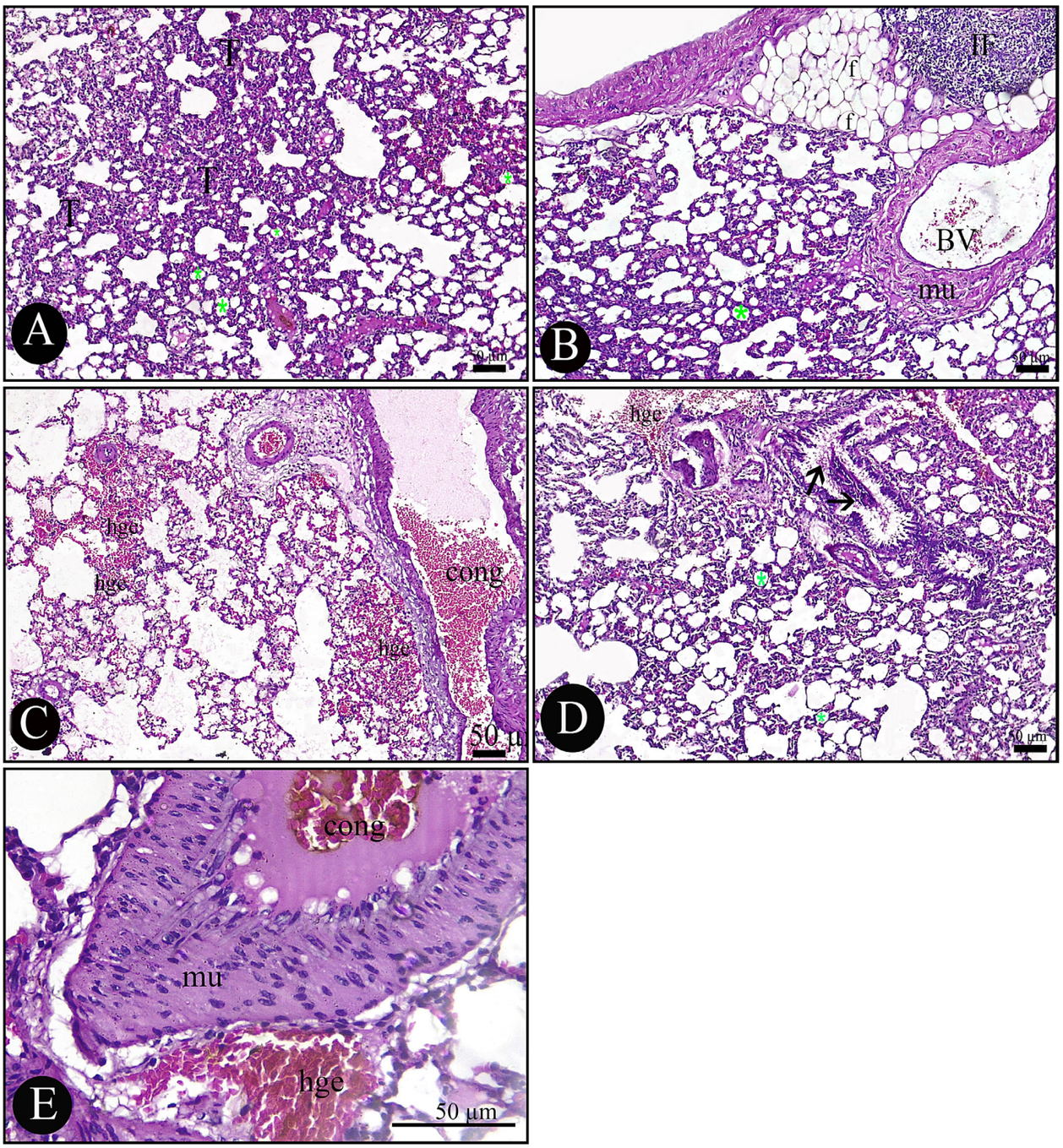

Fig. 2: Photomicrograph of histological sections of H&E slides of experimentally induced asthma group showing: A: Collapsed alveoli (star) with thickened inter-alveolar septa (T). B: Marked inflammatory (IF) and fatty cellular infiltration (f) are observed. Dilated blood vessel (BV) with thick muscle coat (mu) in lung tissue are also well observed. C-E: congestion (cong) and erythrocytes leak in lumina and septa of alveoli forming lung hemorrhage (hge). (D) observed exfoliated bronchial epithelium into the bronchial lumen is obvious (arrow). (E) thick muscle coat of the blood vessel (mu).

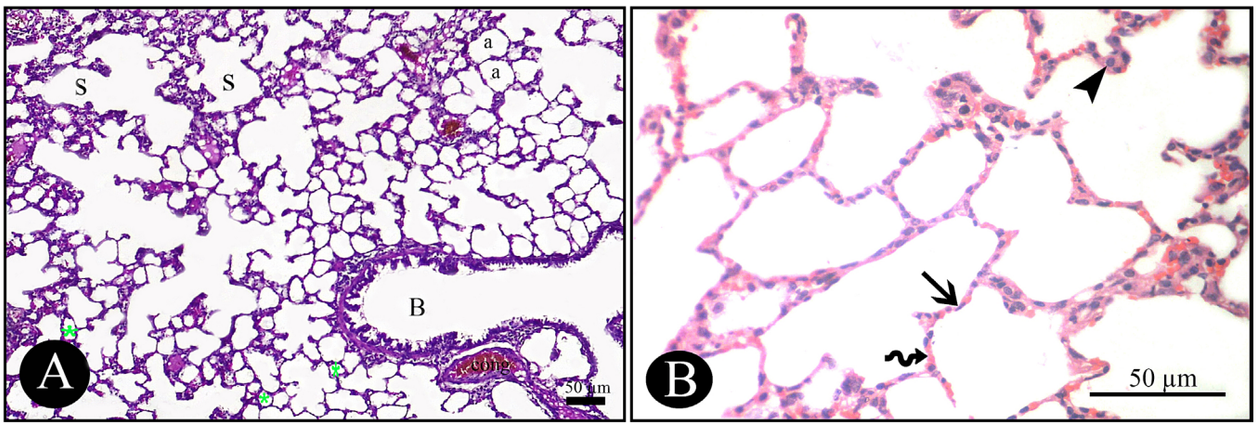

Fig. 3: Photomicrograph of histological sections of H&E slides of exosome-treated group showing (A): alveoli (a), alveolar sacs (s) and bronchiole structure (B) are seen. Some alveoli appear collapsed (star) between the normal alveoli. Notice: congested blood vessel (cong) is seen. (B) The alveoli (a) are aligned by pneumocytes type 1 (arrows) and type 2 (arrow heads). The delicate interalveolar septa (zigzag arrows) separate the alveoli.

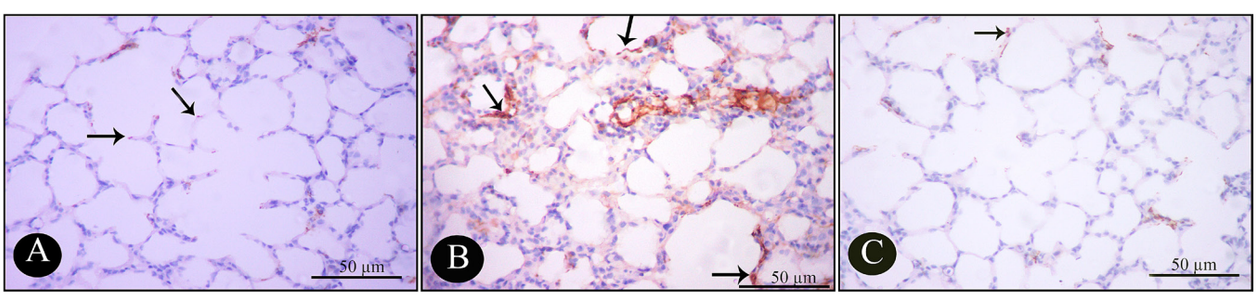

Fig. 4: Immunohistochemically stained lung tissue of albino rats of different groups. brown cytosolic immune representation for NF-κB (arrow). (A): control group: few stained cells. (B): experimentally induced asthma group: Several stained cells. (C): exosome-treated group: few scattered stained cells.

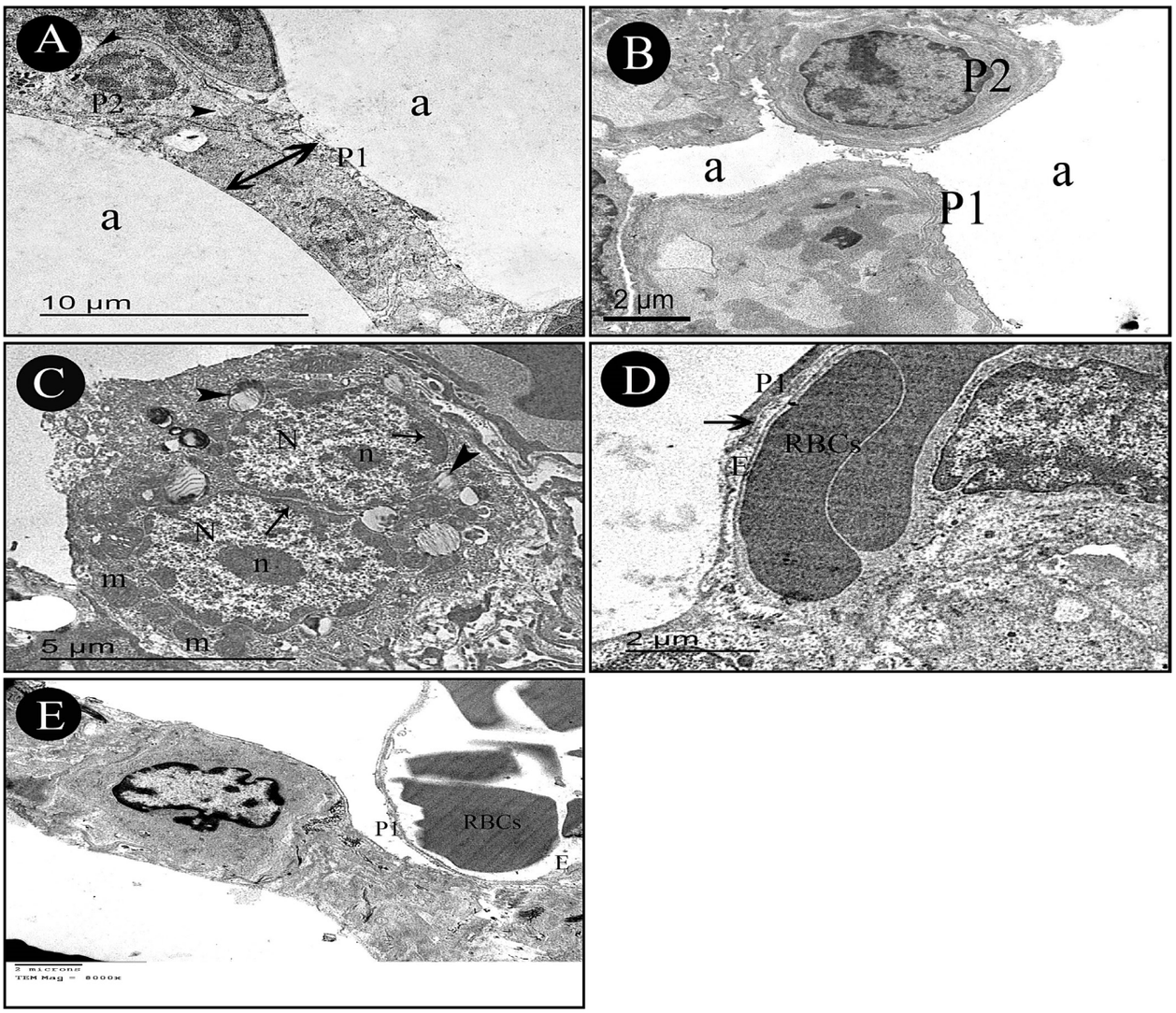

Fig. 5: micrographs of control lung ultrastructure. (A,B) The alveoli (a), type 1 pneumocytes (P1), delicate interalveolar septa (↕) and type 2 pneumocytes (P2). lamellar bodies (arrow head) in its cytoplasm are observed (C) Pneumocytes type 2 (P2) have two regular nuclei (N), peripheral chromatin (arrow) and nucleoli (n). Lamellar bodies (arrowhead), mitochondria (m) are noticed. (D,E) Blood air barrier is made up of thin endothelial cell (E) and type 1 pneumocyte cytosol (P1) with their adherent basal laminae (arrow), Capillary lumen conveys RBCs (R).

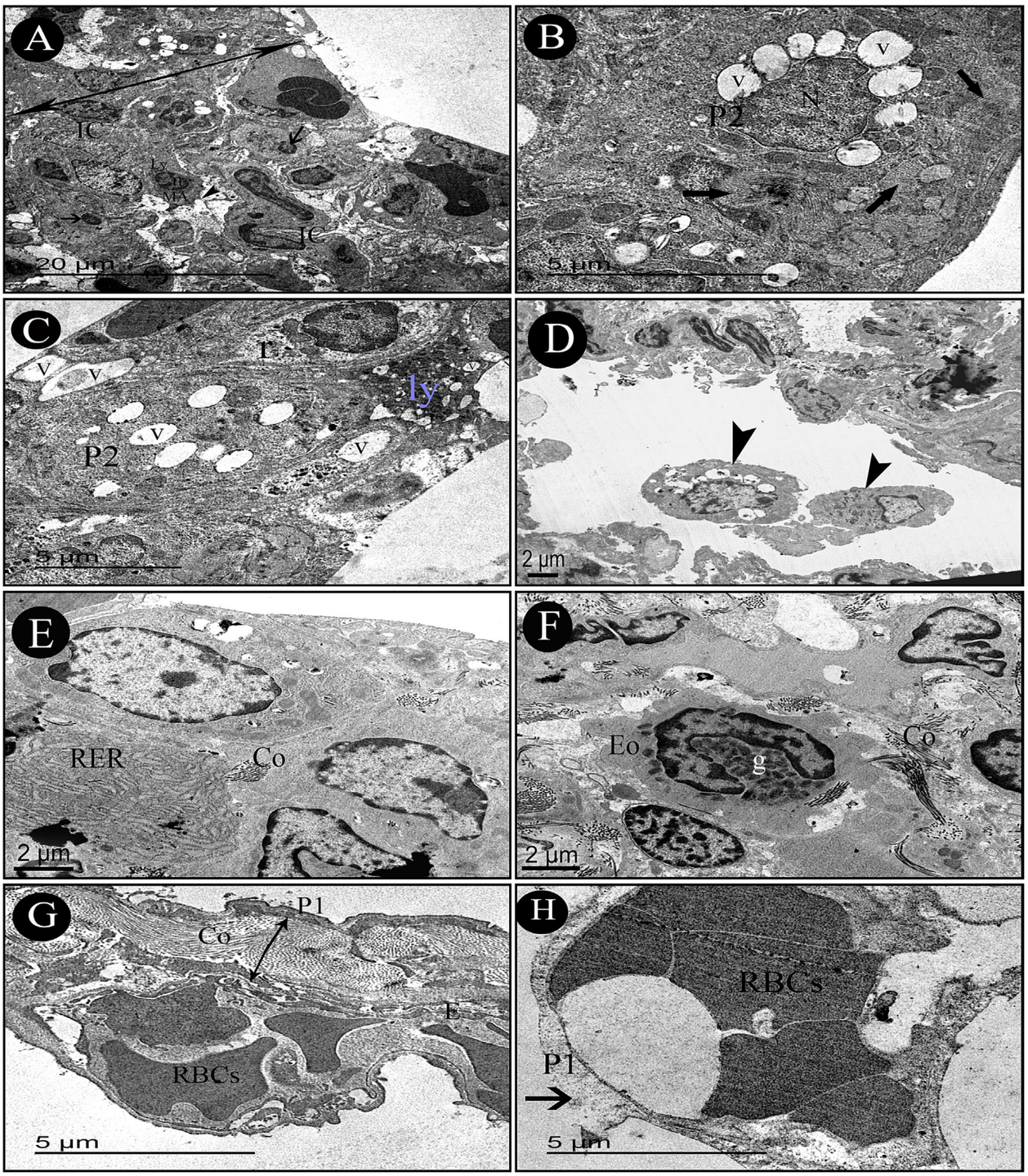

Fig. 6: Micrographs of ultrastructure of lung sections from the experimentally induced asthma group Group. (A) Thick inter-alveolar septa (↕) with many interstitial cells (Ic). Some of them appear with pyknotic degenerated nuclei (arrow). Macrophage (MA) with pseudopodia (arrowhead) and lysosomes (ly) are recognized in inter-alveolar septum. (B) Pneumocyte type 2 (P2) with irregular nucleus (N), empty lamellar bodies (v) are seen. Abundant amount of collagen fibers (thick arrow) is noticed. (C) Many cells appear with rarified cytoplasm (r), vacuolations (v) and lysosomes. (D) Exfoliated cells appear in alveolar lumina (arrow head). (E) Cells appear with dilated RER (RER) and the interstitium contains collagen fibers (Co). (F) Eosinophil (Eo) with its dense granules (g) is noticed in the interstitium which appear with many collagen fibers (Co). (G) Distorted blood air barrier with cytoplasm of pneumocyte type 1 (P1), well separated two basal laminae ( ) containing collagen fibers (Co) and relatively wide irregular cytosol of capillary endothelium (E) is seen. notice: congested blood capillary containing red blood cells (RBCs). (H) Pneumocyte type 1 (P1) has swollen cytoplasm (arrow) and congested blood capillary containing RBCs (RBCs).

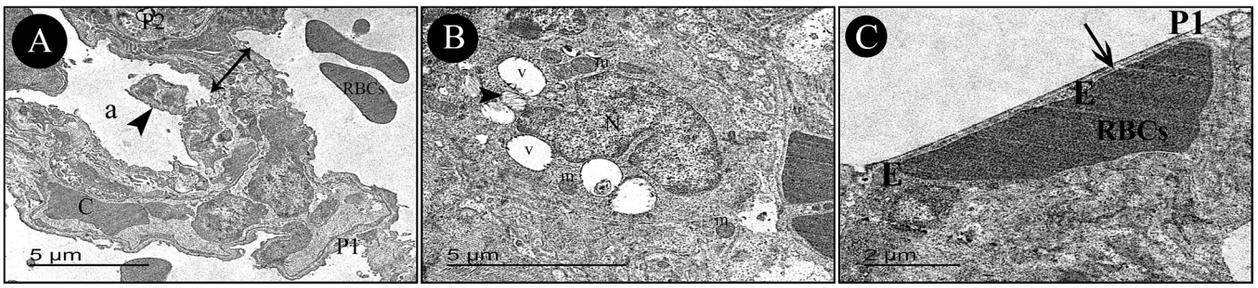

Fig. 7: Micrographs of ultrastructure of lung sections from the exosome-treated group. (A): Apparently normal alveolus (a) with delicate inter-alveolar septum (↕). Pneumocyte type 1 (P1) and 2 (P2) appears with regular nucleus (N). Blood capillary (C) and red blood cells (RBCs) are seen. Notice: leaked cells in the alveolar lumen (arrow head). (B): Pneumocyte type 2 (P2) appears with irregular indented nucleus (N), mitochondria (m) and few lamellar bodies (arrowhead). Some lamellar bodies appear vacuolated (v) (C): A normal blood air barrier is observed. It is made up of thin endothelial cells (E) and type 1 pneumocyte (P1) cytosols, and with their adherent basal laminae (arrow). Capillary lumen conveys RBCs (R).

Table 1: Real-time PCR analysis for miR-146a, interleukin-1 receptor-associated kinase 1 (IRAK1) and nuclear factor kappa B (NF-κB) gene expression in the study groups

Groups	control	experimentally induced asthma	exosome-treated
miR-146a	2.30±0.44	1.36±0.38 [a,b]	2.57±0.40 [NS]
IRAK1	1.77 ±0.34	5.0733± [a,c]	2.0937± [NS]
NF-κB	1.110.20±	2.390.45± [a,c]	1.450.37± [NS]

Values are expressed as mean± standard deviation (SD)
[a] Highly significant difference when comparing experimentally induced asthma group with control group (p<0.001).
[b] significant difference when comparing experimentally induced asthma group with exosome-treated group (p<0.05).
[c] Highly significant difference when comparing experimentally induced asthma group with exosome-treated group (p<0.05). NS Non- significant difference when comparing exosome-treated group with control group (p>0.05)

Table2: Number of anti- NF-κB immune-stained cells.

Groups	control	experimentally induced asthma	exosome-treated
Anti-NF-κB	1.91 ± 0.31	26.77 ± 1.21**	2.95 ± 0.52 *

Values are expressed as mean± standard deviation (SD)
**Highly significant difference when comparing experimentally induced asthma group with both control and exosome-treated groups (p<0.001).
* significant difference when comparing exosome-treated group with control group (p<0.05)

DISCUSSION

Bronchial asthma continues to confuse researchers with its multifaceted pathogenesis and diverse clinical manifestations. Recent research on bronchial asthma has focused on unveiling the pathological complexities of this intriguing chronic respiratory disorder, driving the search for more targeted and personalized therapeutic strategies. The aim was to unravel the ultrastructural and cyto-molecular potential impacts of exosomes extracted from MSCs as biocompatible nanocarriers of miR-146 on experimentally induced bronchial asthma.

H&E-stained tissues of the experimentally induced asthma group displayed collapsed alveoli with thickened inter-alveolar septa. Tohda *et al*.[32] and Zhang *et al*.[33] attributed these disturbances to chronic inflammation, stimulating NF-κB signaling and respiratory tissue remodeling in asthma together with increased mucus production, swelling of airway walls, and constriction of the bronchial smooth muscles. Inflammatory cellular penetration observed in this group, and the appearance of eosinophils within lung tissues trigger the recruitment of various immune cells with subsequent discharge of inflammatory lymphokines. This was adherent to the exfoliation of bronchial epithelium and congested blood vessels with thick muscle coat observed in this group. These detections were linked with Nandedkar *et al*.[34] and Wegmann *et al*.[35], who confirmed that the thickened blood vessels, muscle coat occurred due to chronic inflammation and remodeling processes seen in asthma. Venema *et al*.[36] added that repeated bronchoconstriction, besides chronic inflammatory airway remodeling, steers the sloughing-off process of bronchial epithelium.

Our ultrastructural findings clarified the histopathological observation of the experimentally induced asthma group; we revealed thick inter-alveolar septa and interstitial cells with pyknotic degenerated nuclei. The thickening of inter-alveolar septa with interstitial cells, besides the observation of abundant collagen fibers, proved fibrosis (a common electron microscopy hallmark of chronic inflammation in bronchial asthma). These findings follow

Liu *et al*.[37], who added that these interstitial cells include fibroblasts and myofibroblasts that inked to the excessive generation and deposition of collagen fibers. Moreover, we noticed alveolar macrophages with different lysosomes; Nomura *et al*.[38] confirmed that macrophages enhance the recruitment of activated neutrophils to alveolar spaces, thereby resulting in emerging of IL-4, IL-5, and IL-13 cytokines in broncho-alveolar lavage. Chen *et al*.[39] added that neutrophil extracellular trapping induces macrophages to emit IL-1β, which consecutively promotes neutrophil penetration in the airways. We observed deformed blood-air barriers with separation of the basal lamina, collagen deposition in between, and irregular cytosol of the capillary endothelium; Malmström *et al*.[40] examined lung tissues from severe asthmatic patients and observed increased thickness and discontinuity in the basement membrane, reticular fiber deposition, beside discrepancies in the cytosol of the endothelial cells. Sweerus *et al*.[41] refered that the epithelial α-catenin, E-cadherin, and claudin-18 expression in asthmatic patients links to airway barrier defect and a high influx of TH2, potentially promoting airway hyperresponsiveness. The observed swelling, rarified cytoplasm, and vacuolations of pneumocyte cells in this study align with Li *et al*.[42], who confirmed the alveolar epithelium's thickness and glycoprotein accumulation in these cells. Tan *et al*.[43] explained these findings via the pro-inflammatory effect of fibroblast growth factor 2 revealed in human airway epithelium-derived A549 cells. Over and above, type 2 pneumocyte appeared with irregular nuclei and empty lamellar bodies. Schmiedl *et al*.[44] proved the decline of the surfactant proteins-SP-A and SP-B-containing type 2 pneumocytes and Clara cells in experimental asthma model.

MSCs-derived exosomes, an outstanding means of cellular communication, are promising mediators in tissue repair and modulation of inflammation. Our histopathological results proved restoration of normal bronchiolar and alveolar architecture in the MSCs exosome-treated group. Furthermore, ultrastructural findings clarified this improvement, with restored blood-air barrier integrity and type 1 pneumocytes nanostructure. Yang *et al*.[45] reported that exosomes are now considered a fundamental biological nanoplatform, as they revealed increased delivery and curative efficacy because of their biocompatibility and the magnitute to escape degradation.

To further elucidate the underlying mechanisms of how MSCs-derived exosomes exhibit our forementioned results, we assessed miR-146a as a current universally acknowledged anti-inflammatory exosomal cargo with the paucity of research in bronchial asthma. Specifically speaking, in this work, miR-146a representation was significantly rised after MSCs-derived exosomes. Sanada *et al*.[46] reported an observable miR146a-induced reduction of IL-6 and MCP-1 in macrophages, adipocytes, and fibroblasts of periodontal tissues. Mortazavi-Jahromi *et al*.[47] proved miR146a immunomodulatory impacts in rheumatoid arthritis patients. Over and above, Huang *et al*.[48] confirmed that miR-146a ameliorated pulmonary inflammation and barrier disturbance by downregulating Toll-like receptor 7 in sepsis-associated acute respiratory distress syndrome.

Namely, IRAK1/NF-κB axis is a regulative target of miR-146a. We recorded observable downregulation of IRAK1 and NF-κB expression in the MSCs exosomes-treated group relative to experimentally induced asthma group by Real-time qPCR. Moreover, immunohistochemical representation of NF-κB in our results was also reduced in the MSCs exosomes-treated group. He *et al*.[49] proved that miR-146a representation enhanced the anti-apoptotic effect caused by dexmedetomidine via declining of IRAK1, Caspase-3, and NF-κB protein levels. Zhou *et al*.[50] explained that miR-146a significantly lowered IRAK1 expression, nuclear p65 levels, and decreased IL-6 and TNF-α levels in sensitized THP-1 cells. Furthermore, miR-146a inhibited NF- κB bracing and pro-inflammatory cytokine emergence, proving the regulatory role of miR-146a in systemic lupus inflammatory response. Additionally, Wu *et al*.[51] studied exosomal miR-146a impacts on TNBS-induced colitis, which significantly inhibited TNF receptor–associated factor 6 and IRAK1, phosphorylation levels of NF-κB, were down-regulated and ameliorated cytomolecular inflammatory response. Furthermore, Su *et al*.[52] assessed that repeated systemic inoculation of miR146a, inhibited NF-κB target genes and prevented activation of downstream signaling incidents in the IRAK1/NF-κB pathway in myeloid cells, thereby inhibiting the inflammatory response and thwarted dissemination of HL-60 leukemia. Interestingly, in a murine model of ovalbumin (OVA)-induced asthma treated with dexmedetomidine, Xiao *et al*.[53] demonstrated a significant drop of NF-κB and phosphorylated NF-κB expression, which alleviated airway hyperresponsiveness via toll-like receptor 4. Over and above, Huang *et al*.[54] confirmed pulmonary anti-inflammatory response induced by respiratory syncytial virus via MAPK/NF-κB signaling pathway after treatment with miR-146a mimic.

CONCLUSION

Our study outlined the curative potential of miRNA-146 in mesenchymal stem cell exosomes via IRAK1/NF-κB pathway as a novel and effective approach for managing bronchial asthma and paving the way for further research.

CONFLICT OF INTERESTS

There are no conflicts of interest.

REFERENCES

1. Kuruvilla, M. E., Lee, F. E. H., & Lee, G. B. (2019). Understanding asthma phenotypes, endotypes, and mechanisms of disease. Clinical reviews in allergy & immunology, 56, 219-233. DOI: 10.1007/s12016-018-8712-1
2. Blumenthal, M. N. (2012). Genetic, epigenetic, and environmental factors in asthma and allergy. Annals of Allergy, Asthma & Immunology, 108(2), 69-73. DOI: 10.1016/j.anai.2011.12.003

3. Kaur, R., & Chupp, G. (2019). Phenotypes and endotypes of adult asthma: moving toward precision medicine. Journal of Allergy and Clinical Immunology, 144(1), 1-12. DOI: 10.1016/j.jaci.2019.05.031

4. Pembrey, L., Barreto, M. L., Douwes, J., Cooper, P., Henderson, J., Mpairwe, H., ... & Pearce, N. (2018). Understanding asthma phenotypes: the World Asthma Phenotypes (WASP) international collaboration. ERJ open research, 4(3). DOI: 10.1183/23120541.00013-2018

5. Du, Q., Meng, W., Athari, S. S., & Wang, R. (2021). The effect of Co-Q10 on allergic rhinitis and allergic asthma. Allergy, Asthma & Clinical Immunology, 17, 1-11. DOI: 10.1186/s13223-021-00534-5

6. Imaoka, H., Hoshino, T., Okamoto, M., Sakazaki, Y., Sawada, M., Takei, S., ... & Aizawa, H. (2009). Endogenous and exogenous thioredoxin 1 prevents goblet cell hyperplasia in a chronic antigen exposure asthma model. Allergology International, 58(3), 403-410. DOI: 10.2332/allergolint.09-OA-0086

7. Papi, A., Blasi, F., Canonica, G. W., Morandi, L., Richeldi, L., & Rossi, A. (2020). Treatment strategies for asthma: reshaping the concept of asthma management. Allergy, Asthma & Clinical Immunology, 16, 1-11. DOI: 10.1186/s13223-020-00472-8

8. Paudel, K. R., Wadhwa, R., Mehta, M., Chellappan, D. K., Hansbro, P. M., & Dua, K. (2020). Rutin loaded liquid crystalline nanoparticles inhibit lipopolysaccharide induced oxidative stress and apoptosis in bronchial epithelial cells in *vitro*. Toxicology in *vitro*, 68, 104961. DOI: 10.1016/j.tiv.2020.104961

9. Reagan, M. R., & Kaplan, D. L. (2011). Concise review: mesenchymal stem cell tumor-homing: detection methods in disease model systems. Stem cells, 29(6), 920-927. DOI: 10.1002/stem.645

10. Uccelli, A., Moretta, L., & Pistoia, V. (2008). Mesenchymal stem cells in health and disease. Nature reviews immunology, 8(9), 726-736. DOI: 10.1038/nri2395

11. Wiest, E. F., & Zubair, A. C. (2020). Challenges of manufacturing mesenchymal stromal cell–derived extracellular vesicles in regenerative medicine. Cytotherapy, 22(11), 606-612. DOI: 10.1016/j.jcyt.2020.04.040

12. Maqsood, M., Kang, M., Wu, X., Chen, J., Teng, L., & Qiu, L. (2020). Adult mesenchymal stem cells and their exosomes: Sources, characteristics, and application in regenerative medicine. Life Sciences, 256, 118002. DOI: 10.1016/j.lfs.2020.118002

13. Van Niel, G., d'Angelo, G., & Raposo, G. (2018). Shedding light on the cell biology of extracellular vesicles. Nature reviews Molecular cell biology, 19(4), 213-228. DOI: 10.1038/nrm.2017.125.

14. Rahmani, A., Saleki, K., Javanmehr, N., Khodaparast, J., Saadat, P., & Nouri, H. R. (2020). Mesenchymal stem cell-derived extracellular vesicle-based therapies protect against coupled degeneration of the central nervous and vascular systems in stroke. Ageing Research Reviews, 62, 101106. DOI: 10.1016/j.arr.2020.101106.

15. Piper, R. C., & Katzmann, D. J. (2007). Biogenesis and function of multivesicular bodies. Annu. Rev. Cell Dev. Biol., 23, 519-547. DOI: 10.1146/annurev.cellbio.23.090506.123319.

16. Verdera, H. C., Gitz-Francois, J. J., Schiffelers, R. M., & Vader, P. (2017). Cellular uptake of extracellular vesicles is mediated by clathrin-independent endocytosis and macropinocytosis. Journal of Controlled Release, 266, 100-108. DOI: 10.1016/j.jconrel.2017.09.019.

17. Cai, Y., Yu, X., Hu, S., & Yu, J. (2009). A brief review on the mechanisms of miRNA regulation. Genomics, proteomics & bioinformatics, 7(4), 147-154. DOI: 10.1016/S1672-0229(08)60044-3

18. Bavelloni, A., Ramazzotti, G., Poli, A., Piazzi, M., Focaccia, E., Blalock, W., & Faenza, I. (2017). MiRNA-210: a current overview. Anticancer research, 37(12), 6511-6521. DOI: 10.21873/anticanres.12107.

19. Bekris, L. M., & Leverenz, J. B. (2015). The biomarker and therapeutic potential of miRNA in Alzheimer's disease. Neurodegenerative disease management, 5(1), 61-74. DOI: 10.2217/nmt.14.52

20. Goh, S. Y., Chao, Y. X., Dheen, S. T., Tan, E. K., & Tay, S. S. W. (2019). Role of MicroRNAs in Parkinson's disease. International journal of molecular sciences, 20(22), 5649. DOI: 10.3390/ijms20225649

21. Gandhi, R. (2015). miRNA in multiple sclerosis: search for novel biomarkers. Multiple Sclerosis Journal, 21(9), 1095-1103. DOI: 10.1177/1352458515578771

22. Ma, Y. (2018). The challenge of microRNA as a biomarker of epilepsy. Current Neuropharmacology, 16(1), 37-42. DOI: 10.2174/1570159X15666170703102410

23. Ji, L., Hou, X., Liu, W., Deng, X., Jiang, Z., Huang, K., & Li, R. (2018). Paeoniflorin inhibits activation of the IRAK1-NF-κB signaling pathway in peritoneal macrophages from lupus-prone MRL/lpr mice. Microbial Pathogenesis, 124, 223-229. DOI: 10.1016/j.micpath.2018.08.051

24. Wang, P., Song, D., Wan, D., Li, L., Mei, W., Li, X., ... & Zhang, R. (2020). Ginsenoside panaxatriol reverses TNBC paclitaxel resistance by inhibiting the IRAK1/NF-κB and ERK pathways. PeerJ, 8, e9281. DOI: 10.7717/peerj.9281

25. Woo, L. N., Guo, W. Y., Wang, X., Young, A., Salehi, S., Hin, A., ... & Chow, C. W. (2018). A 4-week model of house dust mite (HDM) induced allergic airways inflammation with airway remodeling. Scientific Reports, 8(1), 1-11. DOI: 10.1038/s41598-018-24574-x

26. Xin, H., Li, Y., Cui, Y., Yang, J. J., Zhang, Z. G., & Chopp, M. (2013): Systemic administration of exosomes released from mesenchymal stromal cells promote functional recovery and neurovascular plasticity after stroke in rats. Journal of Cerebral Blood Flow & Metabolism, 33(11), 1711-1715. DOI: 10.1038/jcbfm.2013.152

27. Thery C, Amigorena S, Raposo G, Clayton A. (2006): Isolation and characterization of exosomes from cell culture supernatants and biological fluids. Curr. Protoc. Cell Biol. 2006;Chapter 3:Unit 3.22. DOI: 10.1002/0471143030.cb0322s30

28. Dobhal, S.; Baliyan, S.; Singh, M. F.; Bisht, S. and Setya, S. (2021): Amelioration of the Abnormalities Associated with Metabolic Syndrome by L-Norvaline in Hyperlipidemic Diabetic Rats. European Pharmaceutical Journal, 68(2), 16-26. DOI: https://doi.org/10.2478/afpuc-2021-0015

29. Kiernan, J. A. (2015): Histological and Histochemical Methods: Theory and Practice 5th Ed. (Banbury: Scion Publishing Ltd; 2015). DOI: 10.1111/joa.12390

30. Ramos-Vara, J. A. *et al*. American association of veterinary laboratory diagnosticians subcommittee on standardization of immunohistochemistry suggested guidelines for immunohistochemical techniques in veterinary diagnostic laboratories. J. Vet. Diagn. Invest. 20(4), 393–413 (2008). DOI: 10.1177/104063870802000401

31. Jung, M. K., & Mun, J. Y. (2018). Sample preparation and imaging of exosomes by transmission electron microscopy. JoVE (Journal of Visualized Experiments), (131), e56482. DOI: 10.3791/56482

32. Tohda, Y., Kubo, H., Ito, M., Fukuoka, M., & Nakajima, S. (2001). Histopathology of the airway epithelium in an experimental dual-phase model of bronchial asthma. Clinical & Experimental Allergy, 31(1), 135-143. doi.org/10.1111/j.1365-2222.2001.01039.x

33. Zhang, B., Wang, B., Cao, S., Wang, Y., & Wu, D. (2017). Silybin attenuates LPS-induced lung injury in mice by inhibiting NF-κB signaling and NLRP3 activation. International Journal of Molecular Medicine, 39(5), 1111-1118. https://doi.org/10.3892/ijmm.2017.2935

34. Nandedkar, S. D., Feroah, T. R., Hutchins, W., Weihrauch, D., Konduri, K. S., Wang, J., ... & Pritchard, K. A. (2008). Histopathology of experimentally induced asthma in a murine model of sickle cell disease. Blood, The Journal of the American Society of Hematology, 112(6), 2529-2538. DOI: 10.1182/blood-2008-01-132506

35. Wegmann, M., Fehrenbach, H., Fehrenbach, A., Held, T., Schramm, C., Garn, H., & Renz, H. (2005). Involvement of distal airways in a chronic model of experimental asthma. Clinical & Experimental Allergy, 35(10), 1263-1274. DOI: 10.1111/j.1365-2222.2005.02306.x

36. Venema, C. M., Williams, K. J., Gershwin, L. J., Reinero, C. R., & Carey, S. A. (2013). Histopathologic and morphometric evaluation of the nasal and pulmonary airways of cats with experimentally induced asthma. International Archives of Allergy and Immunology, 160(4), 365-376. DOI: 10.1159/000342992

37. Liu, J. N., Suh, D. H., Trinh, H. K. T., Chwae, Y. J., Park, H. S., & Shin, Y. S. (2016). The role of autophagy in allergic inflammation: a new target for severe asthma. Experimental & Molecular Medicine, 48(7), e243-e243. DOI: 10.1038/emm.2016.38

38. Nomura, H., Sato, E., Koyama, S., Haniuda, M., Kubo, K., Nagai, S., & Izumi, T. (2001). Histamine stimulates alveolar macrophages to release neutrophil and monocyte chemotactic activity. Journal of Laboratory and Clinical Medicine, 138(4), 226-235. DOI: 10.1067/mlc.2001.117988

39. Chen, X., Li, Y., Qin, L., He, R., & Hu, C. (2021). Neutrophil extracellular trapping network promotes the pathogenesis of neutrophil-associated asthma through macrophages. Immunological investigations, 50(5), 544 561. DOI: 10.1080/08820139.2020.1778720

40. Malmström, K., Lohi, J., Sajantila, A., Jahnsen, F. L., Kajosaari, M., Sarna, S., & Mäkelä, M. J. (2017). Immunohistology and remodeling in fatal pediatric and adolescent asthma. Respiratory Research, 18, 1-9. DOI: 10.1186/s12931-017-0575-0.

41. Sweerus, K., Lachowicz-Scroggins, M., Gordon, E., LaFemina, M., Huang, X., Parikh, M., ... & Frank, J. A. (2017). Claudin-18 deficiency is associated with airway epithelial barrier dysfunction and asthma. Journal of Allergy and Clinical Immunology, 139(1), 72-81. DOI: 10.1016/j.jaci.2016.02.035

42. Li, Z., Liu, Z., Uddandrao, V. S., Ponnusamy, P., Balakrishnan, S., Brahmanaidu, P., ... & Ganapathy, S. (2019). Asthma-alleviating potential of 6-gingerol: effect on cytokines, related mRNA and c-Myc, and NFAT1 expression in ovalbumin-sensitized asthma in rats. Journal of Environmental Pathology, Toxicology and Oncology, 38(1). DOI: 10.1615/JEnvironPatholToxicolOncol.2018027172

43. Tan, Y. Y., Zhou, H. Q., Lin, Y. J., Yi, L. T., Chen, Z. G., Cao, Q. D., ... & Yan, Y. (2022). FGF2 is overexpressed in asthma and promotes airway inflammation through the FGFR/MAPK/NF-κB pathway in airway epithelial cells. Military Medical Research, 9(1), 1-16. DOI: 10.1186/s40779-022-00366-3

44. Schmiedl, A., Tschernig, T., Brasch, F., Pabst, R., & Bargsten, G. (2005). Decrease of the surface fraction of surfactant proteins containing Clara cells and type II pneumocytes in a rat asthma model. Experimental and Toxicologic Pathology, 56(4-5), 265-272. DOI: 10.1016/j.etp.2004.10.004.

45. Yang, B., Chen, Y., & Shi, J. (2019). Exosome biochemistry and advanced nanotechnology for next-generation theranostic platforms. Advanced Materials, 31(2), 1802896. DOI: 10.1002/adma.201802896

46. Sanada, T., Sano, T., Sotomaru, Y., Alshargabi, R., Yamawaki, Y., Yamashita, A., ... & Nishimura, F. (2020). Anti-inflammatory effects of miRNA-146a induced in adipose and periodontal tissues. Biochemistry and biophysics reports, 22, 100757.s DOI: 10.1016/j.bbrep.2020.100757

47. Mortazavi-Jahromi, S. S., Ahmadzadeh, A., Rezaieyazdi, Z., Aslani, M., Omidian, S., & Mirshafiey, A. (2020). The role of β-d-mannuronic acid, as a new non-steroidal anti-inflammatory drug on expression of miR-146a, IRAK1, TRAF6, NF-κB and pro-inflammatory cytokines following a clinical trial in rheumatoid arthritis patients. Immunopharmacology and Immunotoxicology, 42(3), 228-236. DOI: 10.1080/08923973.2020.1742734

48. Huang, H., Zhu, J., Gu, L., Hu, J., Feng, X., Huang, W., ... & Zou, L. (2022)a. TLR7 mediates acute respiratory distress syndrome in sepsis by sensing extracellular miR-146a. American Journal of Respiratory Cell and Molecular Biology, 67(3), 375-388. DOI: 10.1165/rcmb.2021-0551OC

49. He, L., Wang, Z., Zhou, R., Xiong, W., Yang, Y., Song, N., & Qian, J. (2021). Dexmedetomidine exerts cardioprotective effect through miR-146a-3p targeting IRAK1 and TRAF6 via inhibition of the NF-κB pathway. Biomedicine & Pharmacotherapy, 133, 110993. DOI: 10.1016/j.biopha.2020.110993

50. Zhou, C., Zhao, L., Wang, K., Qi, Q., Wang, M., Yang, L., ... & Mu, H. (2019). MicroRNA 146a inhibits NF κB activation and pro inflammatory cytokine production by regulating IRAK1 expression in THP 1 cells. Experimental and therapeutic medicine, 18(4), 3078-3084. DOI: 10.3892/etm.2019.7881

51. Wu, H., Fan, H., Shou, Z., Xu, M., Chen, Q., Ai, C., ... & Liu, X. (2019). Extracellular vesicles containing miR-146a attenuate experimental colitis by targeting TRAF6 and IRAK1. International immunopharmacology, 68, 204-212. DOI: 10.1016/j.intimp.2018.12.043

52. Su, Y. L., Wang, X., Mann, M., Adamus, T. P., Wang, D., Moreira, D. F., ... & Kortylewski, M. (2020). Myeloid cell–targeted miR-146a mimic inhibits NF-κB–driven inflammation and leukemia progression in *vivo*. Blood, 135(3), 167-180. DOI: 10.1182/blood.2019002045

53. Xiao, S., Wang, Q., Gao, H., Zhao, X., Zhi, J., & Yang, D. (2022). Dexmedetomidine alleviates airway hyperresponsiveness and allergic airway inflammation through the TLR4/NF κB signaling pathway in mice. Molecular Medicine Reports, 25(3), 1-10. DOI: 10.3892/mmr.2022.12590

54. Huang, Z., Liu, X., Wu, X., Chen, M., & Yu, W. (2022)b. MiR-146a alleviates lung injury caused by RSV infection in young rats by targeting TRAF-6 and regulating JNK/ERKMAPK signaling pathways. Scientific Reports, 12(1), 3481. DOI: 10.1038/s41598-022-07346-6

الملخص العربى

miR-146a بداخل الإكسوسومات المشتقة من الخلايا الجذعية الوسيطة يحسن التركيب الهستولوجي لنسيج الرئة عبر مسار IRAKI/NF-κB بعد احداث الربو القصبي

إيمان مسلم محمد ومي أمين سمك

قسم الهستولوجيا وبيولوجيا الخلية، كلية الطب البشري، جامعة الزقازيق

المقدمة: الربو القصبي هو اضطراب تنفسي متعدد الأوجه يمثل مصدر قلق عالمي كبير على الصحة العامة، حيث يصيب الملايين من الأفراد ويؤدي إلى معدلات مراضة ووفيات كبيرة.

هدف العمل: نحن نهدف إلى الكشف عن التأثيرات المعقدة الهيكلية والجزيئية الخلوية للإكسوسومات الصادرة عن الخلايا الجذعية الصلبة باعتبارها ناقلات نانوية متوافقة حيويًا من miR-١٤٦ على الربو القصبي المستحث تجريبيًا.

المواد والطرق: تم تقسيم اثنين وثلاثين من ذكور الجرذان البيضاء البالغة إلى ثلاث مجموعات. المجموعة الضابطة، ومجموعات الربو المستحث: كل جرذ تلقي ٢٥ ميكروجرام من عث الغبار المذابة في محلول الملح خمس مرات أسبوعيا لمدة أربعة أسابيع عن طريق الأنف والمجموعة المعالجة بالإكسوسوم: عولجت مثل المجموعة الثانية ثم بعد أسبوعين تلقت الجرذان مائة ميكروجرام من الاكسوسومات عن طريق وريد الذيل مرة يوميا لمدة أسبوعين. تم فحص عينات الأنسجة الرئوية للتحقق من التعبير المناعي النسيجي والبنية التحتية وNF-KB بالإضافة إلى تقدير RT-PCR لـ a-miR١٤٦ و IRAK١ وNF. - كيلو بايت.

النتائج: أثبتت نتائجنا استعادة نسيجية وبنية تحتية ملحوظة لهندسة الأنسجة الرئوية في المجموعة المعالجة بالإكسوسومات MSC مقارنة بمجموعات الربو المستحث. علاوة على ذلك، فإن تقليل التنظيم الكبير لـ IRAK١ وNF-κB، إلى جانب تنظيم a-miR١٤٦ ونقص التعبير الهستوكيميائي مناعي للNF-κB في المجموعة المعالجة أشار إلى الآليات الجزيئية المحتملة الكامنة وراء التأثيرات النسيجية المورفومترية المرصودة.

الخلاصة: حددت دراستنا الإمكانات العلاجية لـ miRNA-١٤٦ في إكسوسومات الخلايا الجذعية الوسيطة عبر مسار IRAKI/NF-κB كنهج جديد وفعال لإدارة الربو القصبي وتمهيد الطريق لمزيد من البحث.